mRNA vaccine induces cytotoxic CD8+ T-cell cross-reactivity against SARS-CoV-2 Omicron variant and regulates COVID-19 severity

Takuto Nogimori
National Institutes of Biomedical Innovation, Health and Nutrition https://orcid.org/0000-0002-6011-9631

Koichiro Suzuki
The Research Foundation for Microbial Diseases of Osaka University

Yuji Masuta
National Institutes of Biomedical Innovation, Health and Nutrition https://orcid.org/0000-0003-2349-6320

Mika Yagoto
National Institutes of Biomedical Innovation, Health and Nutrition

Mami Ikeda
National Institutes of Biomedical Innovation, Health and Nutrition

Yuki Katayama
National Institutes of Biomedical Innovation, Health and Nutrition

Ayaka Washizaki
National Institutes of Biomedical Innovation, Health and Nutrition

Hidenori Kanda
KINSHUKAI, Hanwa The Second Hospital

Minoru Takada
KINSHUKAI, Hanwa The Second Senboku Hospital

Shohei Minami
Research Institute for Microbial Diseases, Osaka University

Takeshi Kobayashi
Research Institute for Microbial Diseases, Osaka University

Shokichi Takahama
National Institutes of Biomedical Innovation, Health and Nutrition https://orcid.org/0000-0002-5651-4217

Yasuo Yoshioka
Research Institute for Microbial Diseases, Osaka University https://orcid.org/0000-0002-7265-9221

Takuya Yamamoto (yamamotot2@nibiohn.go.jp)

National Institutes of Biomedical Innovation, Health and Nutrition https://orcid.org/0000-0003-3753-1211

Article

Keywords:

Posted Date: April 11th, 2022

DOI: https://doi.org/10.21203/rs.3.rs-1364513/v1

mRNA vaccine induces cytotoxic CD8$^+$ T-cell cross-reactivity against SARS-CoV-2 Omicron variant and regulates COVID-19 severity

Takuto Nogimori[1,2], Koichiro Suzuki[3], Yuji Masuta[1,4], Mika Yagoto[1], Mami Ikeda[1], Yuki Katayama[1], Ayaka Washizaki[1], Hidenori Kanda[5], Minoru Takada[6], Shohei Minami[7], Takeshi Kobayashi[7], Shokichi Takahama[1,2], Yasuo Yoshioka[3,8,9,10], and Takuya Yamamoto[1,2,4,7,11]*

[1] Laboratory of Immunosenescence, National Institutes of Biomedical Innovation, Health and Nutrition, Osaka, Japan

[2] Research Institute for Microbial Diseases, Osaka University, Osaka, Japan

[3] The Research Foundation for Microbial Diseases of Osaka University (BIKEN), Osaka, Japan

[4] Laboratory of Aging and Immune Regulation, Graduate School of Pharmaceutical Sciences, Osaka University, Osaka, Japan

[5] KINSHUKAI, Hanwa The Second Hospital, Osaka, Japan

[6] KINSHUKAI, Hanwa The Second Senboku Hospital, Osaka, Japan

[7] Department of Virology, Research Institute for Microbial Diseases, Osaka University, Osaka, Japan

[8] Vaccine Creation Group, BIKEN Innovative Vaccine Research Alliance Laboratories, Research Institute for Microbial Diseases, Osaka University, Osaka, Japan

[9] Laboratory of Nano-design for innovative drug development, Graduate School of Pharmaceutical Sciences, Osaka University, Osaka, Japan

[10] Institute for Open and Transdisciplinary Research Initiatives, Osaka University, Osaka, Japan

[11] Department of Virology and Immunology, Graduate School of Medicine, Osaka University, Osaka, Japan.

* Corresponding author

Takuya Yamamoto

Laboratory of Immunosenescence

National Institutes of Biomedical Innovation, Health and Nutrition

7-6-8, Saito-Asagi, Ibaraki City, Osaka 567-0085, Japan

Email: yamamotot2@nibiohn.go.jp

ABSTRACT

Understanding the T-cell responses involved in inhibiting COVID-19 severity is crucial for developing new therapeutic and vaccine strategies. Here, we characterized SARS-CoV-2 spike-specific $CD8^+$ T cells interacting with overlapping peptides on peripheral blood mononuclear cells from acute-phase COVID-19 patients. Relative to severe COVID-19, patients with mild COVID-19 had more frequent antigen-specific $CD8^+$ T cells, and significantly increased SARS-CoV-2 spike-specific $CD8^+$ T cells simultaneously expressing granzyme A, granzyme B, and perforin, suggesting that inducing highly cytotoxic $CD8^+$ T cells during early infection suppresses COVID-19 severity. The BNT162b2 mRNA vaccine induced these antigen-specific $CD8^+$ T cells in healthy donors, although lesser than in infected patients, and the induced subpopulation was not maintained long-term after second vaccination. Importantly, these $CD8^+$ T cells showed cross-reactivity with the Delta and Omicron strains of SARS-CoV-2. Incorporating factors that efficiently induce $CD8^+$ T cells with polyfunctional cytotoxic activity may improve future vaccine efficacy against such variants.

Introduction

COVID-19, an infectious disease caused by severe acute respiratory syndrome coronavirus 2 (SARS-CoV-2), is an ongoing global pandemic with increasing incidence and mortality[1]. SARS-CoV-2 infection causes a wide variety of clinical features, ranging from asymptomatic cases to severe cases with an inflammatory response and death[2, 3]. The mortality rate of COVID-19 is lower than that of severe acute respiratory syndrome coronavirus (SARS-CoV) and Middle East respiratory syndrome coronavirus (MERS-CoV), but much higher than that of seasonal influenza[4, 5]. The emergence of new variants of concern (VoCs) may further increase disease severity. Indeed, it was suggested that variant B.1.1.7, the Alpha strain, first detected in the UK in September 2020, may cause more severe illness than pre-existing variants[6]. B.1.351 (the Beta strain, detected in South Africa[7]), which has the E484K mutation in the spike-protein receptor-binding domain, shows high resistance to vaccine-induced and anti-monoclonal antibodies[8-11]. Like the Beta strain, the Delta strain, B.1.617.2 (first detected in India in December 2020) also reduces vaccine efficacy; by mid-April 2021 it was the most commonly reported variant in India, and rapidly spread globally[12]. B.1.1.529 (the Omicron strain, which emerged in South Africa in November 2021[13]), has many amino acid mutations in its spike protein, and 15 mutations in the ACE2 receptor-binding domain[14]. Compared to previous VoCs, Omicron more severely reduced vaccine and monoclonal antibody efficacy[14-24]. Furthermore, due to its higher transmissibility, there are concerns about faster and wider spread of SARS-CoV-2 infection[25].

T cells are critical in eliminating many respiratory tract infections in acute phase[26]. Cytotoxic $CD8^+$ T cells, which play a protective role in immune surveillance against viral infection, are an important component of vaccine-induced protective immunity[27]. The induction of cellular and humoral immunity in response to COVID-19 is important in suppressing symptom severity[28, 29]. Lymphopenia is associated with COVID-19 disease severity[30], and the depletion of $CD8^+$ T cells, but not $CD4^+$ T cells, is associated with poor prognosis of COVID-19 patients[31]. In SARS-CoV-2-infected ACE2-transgenic mice with depleted $CD8^+$ T-cell population, the viral load in the lungs elevated 5 d post-infection[32], suggesting that $CD8^+$ T cells play an important role in the early clearance of SARS-CoV-2. In rhesus monkeys with prior SARS-CoV-2 infection, $CD8^+$ T cell depletion reduced their

resistance to SARS-CoV-2 re-challenge[33]. Analysis of SARS-CoV-2-specific T-cell responses in asymptomatic and symptomatic SARS-CoV-2-infected individuals revealed equivalent frequencies of antigen-specific T cells, although asymptomatic individuals had elevated IFN-γ and IL-2 production. While antigen-specific T-cell IFN-γ production and IL-10 and pro-inflammatory cytokine (IL-6, TNF-α, and IL-1β) production were proportionate in asymptomatic individuals, their secretion was disproportionate in symptomatic individuals[34]. In a longitudinal study of SARS-CoV-2-infected patients, from onset to recovery or death, IFN-γ-secreting SARS-CoV-2-specific T cells were induced earlier in individuals with mild disease than in those with severe disease[29]. Indeed, early functional induction of SARS-CoV-2-specific T cells influences COVID-19 patient prognosis.

mRNA vaccines expressing the SARS-CoV-2 spike protein, such as mRNA-1273 (Moderna, Cambridge, MA) and BNT162b2 (Pfizer, New York, NY), which induce antigen-specific T-cell responses[35-37], are currently being used worldwide against COVID-19. They cause remarkable induction of $CD4^+$ T-cell responses, and rapid Th1 and peripheral Tfh cell induction after initial vaccination is associated with $CD8^+$ T-cell responses and antibody induction after second vaccination[38]. Furthermore, although mRNA-vaccine-induced antibody population declines over time, it persists for at least six months[39, 40]. The mRNA-vaccine-induced antigen-specific $CD4^+$ T cell frequency remained stable from three to six months after vaccination, with a half-life of 187 days[41]. In another study, the frequency of $CD4^+$ T cells induced by low-dose mRNA-1273 was maintained even after six months[42]. In contrast, the frequency of $CD8^+$ T cells induced by mRNA vaccines decreased after six months[41].

Despite of increasing evidence on the dynamics of mRNA vaccine-induced cellular immunity, it remains to be clarified which vaccine-induced T-cell responses better predict protection from disease after SARS-CoV-2 exposure. Furthermore, to respond appropriately to new VoCs, it is necessary to determine mRNA vaccine-induced T-cell cross-reactivity to them. T-cell immunity induced by infection or vaccination may be cross-reactive to mutant strains[43-48]. T-cell responses to newly emerged omicron strains have been actively analyzed. For instance, BNT162b2-vaccinated individuals, and those who had recovered from SARS-CoV-2 infection, had antigen-specific T cells

98 that were cross-reactive to the Omicron variant spike protein[49-51]. In vaccine- or infection-induced
99 $CD4^+$ and $CD8^+$ T cells, exposure to the Omicron-derived Spike-peptide pool, or wild-type spike-
100 protein peptides, caused comparable IFN-γ, IL-2, and TNF cytokine production[52].

101 Nonetheless, it remains unclear how the mRNA vaccine-induced cytotoxicity of cross-reactive T cells
102 changes over time. To address this in the present study, we first analyzed peripheral blood
103 mononuclear cells (PBMCs) obtained from 30 symptomatic SARS-CoV-2-infected patients, to
104 identify $CD8^+$ T cell phenotypes that suppress COVID-19 progression. Since $CD8^+$ T cells show
105 antiviral effects mainly by secreting cytotoxic granules[53, 54], we examined the cytotoxicity of SARS-
106 CoV-2 spike-specific $CD8^+$ T cells: in patients with mild disease, there was a high frequency of
107 subpopulations simultaneously expressing granzyme A (GZMA), granzyme B (GZMB), and perforin,
108 indicating the induction of highly functional $CD8^+$ T cells. Next, we examined whether highly
109 cytotoxic $CD8^+$ T cells were induced by BNT162b2 vaccines. One month after the second BNT162b2
110 vaccination, subpopulations simultaneously expressing GZMA, GZMB, and perforin were observed,
111 although at lower frequently than that in naturally infected individuals. The subpopulation frequency
112 did not differ for the Delta and Omicron strains, which differ from the vaccine strain, indicating that
113 the mRNA vaccine-induced antigen-specific but cross-reactive $CD8^+$ T cells. Nonetheless, the
114 frequencies of this subpopulation decreased three months after the second vaccination, suggesting that
115 highly functional antigen-specific $CD8^+$ T cells are not maintained in the long term.

Results

Acute phase SARS-CoV-2 spike-specific $CD8^+$ T-cell response associated with COVID-19 severity

To characterize the $CD8^+$ T cells associated with COVID-19 severity, we enrolled 30 patients infected with Alpha variant of SARS-CoV-2 (Table 1). For the acute-phase, the viral load and anti-spike IgG titer were significantly negatively correlated (Fig. 1a), whereas the antibody titer was not associated with COVID-19 severity (Fig. 1b). Next, we analyzed the SARS-CoV-2 spike-specific $CD8^+$ T cells using flow cytometry. A representative gating scheme for flow cytometric analysis is presented in Extended Data Figure 1. The surface markers CD27 and CD45RO were used to define the total memory-cell population, and CD69 and 4-1BB were used to define an antigen-specific-stimulated population (Fig. 1c). $CD69^+4\text{-}1BB^+CD8^+$ T-cell frequency was significantly higher in patients with mild disease compared to patients with moderate II/severe disease (Fig. 1d), suggesting that antigen-specific $CD8^+$ T cells prevent the progression of COVID-19 pathology.

Functional characteristics of SARS-CoV-2 spike-specific $CD8^+$ T cells in acute COVID-19

Next, to further characterize antigen-specific $CD8^+$ T cells with respect to COVID-19 inhibition, we calculated the cytokine production of $CD8^+$ T cells responding to SARS-CoV-2 spike antigen. IFN-γ, TNF, and IL-2 expression did not vary significantly with severity (Fig 2a and Extended Data Fig 2). The SARS-CoV-2 spike-specific $CD8^+$ T-cell functional profile was not associated with COVID-19 severity (Fig. 2b).

We next evaluated the cytotoxic activity of SARS-CoV-2 spike-specific $CD8^+$ T cells. Most of the $CD69^+4\text{-}1BB^+CD8^+$ T cells expressed granzyme A (GZMA), granzyme B (GZMB) and perforin expression tended to decrease with disease severity (Fig 2c and Extended Data Fig 3).

Simultaneous expression of different cytotoxic molecules is potentially characteristic of effector cells with strong cytotoxicity. Therefore, we analyzed the simultaneous expression of GZMA, GZMB, and perforin in $CD69^+4\text{-}1BB^+CD8^+$ T cells (Fig. 2d). The frequency of subpopulations expressing GZMA,

GZMB, and perforin decreased substantially (by 27%) with COVID-19 severity. Moreover, the frequencies of the simultaneously expressed cytotoxic molecules differed significantly between the mild and moderate II/severe disease groups (Fig. 2e). These results suggest that in the acute phase of COVID-19 pathogenesis, polyfunctional cytotoxic $CD8^+$ T-cell induction is associated with the control of disease progression.

mRNA vaccine induced antibodies and $CD4^+$ T cells against SARS-CoV-2 variants of concern

To measure mRNA vaccine-induced immune responses against SARS-CoV-2 variants of concern, we enrolled 21 healthy adults vaccinated with Pfizer BNT162b2, and obtained samples at three time points: pre-vaccination, four weeks after second vaccination, and twelve weeks after second vaccination. First, we measured the anti-spike IgG endpoint titer in response to wild-type (WT), Delta, and Omicron spikes in plasma samples by performing ELISA (Fig. 3a). At four weeks post-sevond vaccination, antibody titers were high for all spike types (WT, Delta, and Omicron), but lowered twelve weeks post-booster vaccination, consistent with previous reports[41, 55]. At each time point, antibody titers were significantly lower in response to Delta and Omicron spikes than to the WT (Fig. 3b). In particular, four weeks post-booster vaccination, the antibody endpoint titer was 84% lower against the Omicron spike than that against the WT.

To evaluate the role of T cells in protecting against SARS-CoV-2 VoCs exposure, we used flow cytometric analysis to examine $CD4^+$ T cell responses to Delta and Omicron, the recently emerged VoCs of SARS-CoV-2. PBMCs from BNT162b2-vaccinated healthy donors were stimulated with WT, Delta, or Omicron strain-derived spike peptides. Antigen-specific Th1 cells were defined as $CD4^+$ total memory T cells expressing CD154 and IFN-γ (gating scheme shown in Extended Data Fig. 4a). Antigen-specific Th1 cell frequencies were calculated in stimulated samples by subtracting background of unstimulated samples: relative to the response to the WT, antigen-specific Th1 cell frequency was slightly lower in response to the Omicron variant, but not to the Delta variant (Fig. 3c). We evaluated the correlations between the antibody titers and Th1 cell frequencies: the Th1 cell frequency and the anti-spike endpoint titer were significantly correlated (Fig. 3d), suggesting that

mRNA vaccine-mediated induction of Th1 cells is necessary to induce antibodies against VoCs. These results suggest that the response of antigen-specific $CD4^+$ T cells is slightly lower to Omicron than to the WT; however, these cells are maintained for at least three months after the second vaccination.

The mRNA vaccine induces $CD8^+$ T cells against SARS-CoV-2 variants of concern

We next examined whether these antigen-specific $CD8^+$ T cells are induced by the mRNA vaccine, and whether memory T cells are maintained for a long period. The gating scheme was as shown in Figure 1, and the representative plots are shown in Extended Data Figure 4b. $CD69^+4\text{-}1BB^+CD8^+$ T cells were induced by the mRNA vaccine, and their frequencies were maintained for at least twelve weeks post-second vaccination (Fig. 4a). Furthermore, the frequency of $CD69^+4\text{-}1BB^+CD8^+$ T cells did not differ significantly in response to the WT, Delta, and Omicron variants, suggesting that mRNA vaccine-induced antigen-specific $CD8^+$ T cells cross-react with SARS-CoV-2 VoCs.

Cytokine production by $CD8^+$ T cells responding to SARS-CoV-2 spike peptides was low and difficult to quantify (Extended Data Figure 5). To analyze antigen-specific $CD8^+$ T cell cytotoxicity, we evaluated the expression of cytotoxicity-related molecules in $CD69^+4\text{-}1BB^+CD8^+$ T cells responding to VoCs at four and twelve weeks after the second vaccination. GZMA was overexpressed in the $CD69^+4\text{-}1BB^+CD8^+$ T cells of the vaccinated individuals, as well as in the acute phase of the infected individuals (Fig. 4b, left panels). However, relative to their expression at four weeks, expression at twelve weeks post-second vaccination was significantly lower for GZMA (Fig. 4b, left panels), GZMB, and perforin (Fig. 4b, center and right panels). Next, we evaluated the cytotoxicity spectrum of the $CD69^+4\text{-}1BB^+CD8^+$ T cells from vaccinated individuals. The frequency of the T-cell subpopulation simultaneously expressing GZMA, GZMB, and perforin was moderate in vaccinated individuals at four weeks post-second vaccination, whereas it was high in mildly infected donors (Fig. 4c). Furthermore, at twelve weeks post-second vaccination, the frequency of this subpopulation was significantly lower than that at four weeks (Figs 4c, d), suggesting that mRNA-induced antigen-specific $CD8^+$ T cell cytotoxicity is not long-lasting. In contrast, antigen-specific $CD8^+$ T-cell

cytotoxicity did not differ significantly among the VoCs (Delta and Omicron) and the WT strain, indicating that mRNA vaccine-induced $CD8^+$ T cells cross-react with various VoCs.

Discussion

SARS-CoV-2, which first emerged in 2019 in Wuhan, China, is still raging globally. The mRNA vaccines developed to fight this pandemic, now used worldwide, were approved in a shorter-than-usual period owing to the urgency of the situation. Hence, their long-term efficacy remained unknown and need to be determined. To do this, we first characterized antigen-specific $CD8^+$ T cells derived from mildly or severely infected individuals upon restimulation with SARS-CoV-2 spike antigen: antigen-specific $CD8^+$ T cells in the acute phase of mild disease simultaneously expressed GZMA, GZMB, and perforin. Healthy BNT162b2 mRNA vaccine recipients also produced this subpopulation of highly cytotoxic $CD8^+$ T cells, but at a lower proportion than that observed in infected individuals. Furthermore, the frequency of this subpopulation was lower three months after the second vaccination than at one month, suggesting that although the mRNA vaccine induce $CD8^+$ T cells that reduce COVID-19 severity, the effect may not be long-lasting.

Expression of cytotoxic molecules in $CD8^+$ T cells changes during the course of SARS-CoV-2 infection and varies between studies, as determined based on bulk analysis of T-cell responses. For instance, GZMB and perforin expression is higher in SARS-CoV-2-infected patients than in healthy donors[56], whereas another study reported that $CD8^+$ T cell GZMA and perforin expression was comparable between healthy individuals and SARS-CoV-2-infected patients[57]. Consistent with our results, a study based on serum levels rather than intracellular expression analysis revealed that GZMA and perforin serum levels are higher in SARS-CoV-2-infected patients with mild symptoms than in healthy individuals and critically-ill patients[58].

Involvement of $CD8^+$ T cells in COVID-19 pathogenesis can be elucidated by analyzing SARS-CoV-2-specific $CD8^+$ T cell characteristics. In a study using HLA-A02 tetramer[59], antigen-specific $CD8^+$ T cells (obtained from COVID-19 acute-phase patients) responding to the $S_{269\text{-}277}$ epitope of the spike protein predominantly belonged to the subpopulation simultaneously expressing GZMA, GZMB,

GZMK, and perforin; however, it remained unclear whether these $CD8^+$ T cells can suppress COVID-19 severity. To elucidate this, we stimulated PBMCs derived from COVID-19 patients with varying severity with overlapping peptides, and characterized the antigen-specific $CD8^+$ T cells via multicolor flow cytometry. Cytokine production from $CD8^+$ T cells in response to antigen stimulation did not differ significantly between mildly and severely infected patients, but the expression of cytotoxic molecules was notably different. Antigen-specific T cell expression of cytotoxic molecules varies with the type of virus[60]. Therefore, our study outcomes showing cytotoxic molecule expression profile during the course of SARS-CoV-2 infection is all the more relevant for developing future strategies to protect against SARS-CoV-2 infection.

COVID-19 pathogenesis may involve immune checkpoint molecules, in addition to cytotoxic molecules. Expression of PD-1, an inhibitory receptor, is reportedly upregulated in SARS-CoV-2-infected patients[61-63], although its role in COVID-19 severity remains controversial. For instance, analysis of SARS-CoV-2 specific $CD8^+$ T cells using the MHC-I multimer[64] showed that PD-1-expressing $CD8^+$ T cells were also likely to express IFN-γ and activation markers such as CD38 and HLA-DR. This indicates that PD-1 expression on $CD8^+$ T cells of COVID-19 patients may reflect their activation rather than exhaustion. In our study, PD-1 expression did not vary with COVID-19 severity. However, further research is needed to elucidate the association between $CD8^+$ T cell exhaustion and COVID-19 progression.

Based on the results of multicolor flow cytometry of SARS-CoV-2 spike-specific $CD8^+$ T cells in PBMCs obtained from healthy BNT162b2 mRNA vaccine recipients, the frequency of the subpopulation simultaneously expressing GZMA, GZMB, and perforin was 21% in $CD69^+$4-$1BB^+CD8^+$ T cells one month after the second vaccination. In the acute phase of COVID-19 mild disease, this frequency was 68%, suggesting less effective induction of highly functional cytotoxic $CD8^+$ T cells in vaccinated individuals than in naturally infected individuals. Three months after the second vaccination, this subpopulation significantly reduced to 15%. Although SARS-CoV-2 spike-specific $CD8^+$ T cells were present three months after vaccination (based on the presence of $CD69^+$ and 4-$1BB^+$ T cells), their functionality declined gradually. Furthermore, consistent with recent

reports[49-51], subpopulation frequency did not differ significantly between cytotoxic $CD8^+$ T cells reactive to the Delta and Omicron strains and those reactive to the vaccine strain, providing further evidence that $CD8^+$ T cells induced by the vaccine are cross-reactive to VoCs although we couldn't evaluate the actual killing activity of these $CD8^+$ T cells.

Our findings suggest that mRNA vaccination induces a subpopulation of $CD8^+$ T cells that may reduce COVID-19 severity. Nonetheless, inducing as well as maintaining this subpopulation for long-term remains challenging. To increase the efficacy of future vaccines against VoCs, it is worth considering incorporating factors that more efficiently induce $CD8^+$ T cells with polyfunctional cytotoxic activity that can remain in system for long-term.

Methods

Human samples

Fifty one individuals (30 individuals infected with SARS-CoV-2 Alpha-variant and 21 BNT162b2-vaccinated healthy individuals) were enrolled in this study (Table 1), and SARS-CoV-2 infection was confirmed by reverse transcription quantitative PCR (RT-qPCR). Viral RNA was isolated using the NucleoSpin RNA Virus (MACHEREY-NAGEL, Düren, Germany), according to the manufacturer's instructions. The viral RNA was reverse-transcribed and quantified using the One Step PrimeScript III RT-qPCR Mix, with UNG (TaKaRa, Maebashi, Japan) according to the Pathogen Detection Manual 2019-nCoV v. 2.9.1 (National Institute of Infectious Diseases in Japan). Disease severity was categorized using a diagnostic guide from the Japanese Ministry of Health, Labour, and Welfare. The study protocol and procedures were reviewed and approved by the institutional ethics committees of the National Institutes of Biomedical Innovation, Health and Nutrition (approval no. 137), Osaka, Japan, and The Research Foundation for Microbial Diseases of Osaka University (approval no. 20-02), Osaka, Japan, and complied with the 1975 Declaration of Helsinki. All participants provided written informed consent for participating in the study. PBMCs were isolated via density gradient centrifugation using BD Vacutainer CPT cell preparation tube with sodium heparin (Becton, Dickinson, and Co., Franklin Lakes, NJ), according to the manufacturer's instructions. PBMCs were immersed in CELLBANKER cell freezing medium (TaKaRa) and stored in liquid nitrogen vapor until analysis.

SARS-CoV-2 spike-specific antibody detection

The plasma levels of total IgG-targeting SARS-CoV-2 spike-specific antibodies were determined via enzyme-linked immunosorbent assay (ELISA). Recombinant spike proteins (WT: Wuhan-1; Alpha: B.1.1.7; Delta: B.1.617.2; and Omicron: B.1.1.529) were obtained from ACROBiosystems (Newark, DE). To calculate spike-specific antibody titers, 96-well plates were coated with SARS-CoV-2 spike protein and incubated overnight at 4 °C. The plates were then washed and incubated for 1 h with blocking buffer, then washed again, and incubated with diluted plasma samples for 2 h at 25 °C. Next,

the plates were washed and incubated with biotinylated anti-human total IgG (BD Biosciences, San Jose, CA) for 1 h. The plates were then washed and incubated with HRP-conjugated streptavidin (Thermo Fisher Scientific, Waltham, MA) for 1 h at room temperature. The plates were then washed and incubated with TMB peroxidase substrate (KPL, Gaithersburg, MD) for color development. After 10 min, 2 mol/l H_2SO_4 was added to each well to stop the reaction. Antibody expression was measured by determining optical density at 450 nm using an Epoch 2 Microplate Spectrophotometer (Agilent, Santa Clara, CA). The antibody endpoint titer was determined using a cutoff value of 0.3.

Flow cytometry analysis

For analyzing SARS-CoV-2 Spike-specific T cells, we performed surface and intracellular cytokine staining of $CD4^+$ and $CD8^+$ T cells. Briefly, PBMCs were incubated in 1 ml RPMI 1640 medium containing 50 U/ml benzonase nuclease (Millipore, Darmstadt, Germany), 10% fetal bovine serum, and penicillin–streptomycin for 2 h. Next, cells were incubated in 200 µl medium with or without peptides (17-mers overlapping by 11 residues) corresponding to the full-length SARS-CoV-2 spike (Supplementary Table 1), at a final concentration of 2 µg/ml of each peptide, for 30 min. Thereafter, 0.2 µl BD GolgiPlug and 0.14 µl BD GolgiStop (both from BD Biosciences) were added and incubated for 5.5 h. The cells were then stained using the LIVE/DEAD Fixable Blue Dead Cell Stain Kit (Thermo Fisher Scientific), and stained with anti-CD3 (SP34-2), anti-CD8 (RPA-T8), anti-CD4 (L200), anti-CD45RO (UCHL1), anti-CD27 (1A4CD27), and anti-PD-1 (EH12-2H7) antibodies. After fixation and permeabilization using the Cytofix/Cytoperm kit (BD Biosciences), the cells were stained with anti-4-1BB (4B4-1), anti-CD69 (FN50), and anti-IFN-γ (4S.B3), anti-TNF (MAb11), anti-IL-2 (MQ-17H12), anti-granzyme A (CB9), anti-granzyme B (GB11), and anti-perforin (B-D45) antibodies. Cells were analyzed using a BD FACSymphony A5 flow cytometer (BD Biosciences). The data were analyzed using FlowJo v. 10.8.1.

Statistical Analysis

Data were analyzed using GraphPad Prism 9. *P*-values were determined using the nonparametric Mann-Whitney *U* test and Wilcoxon matched-pairs signed-rank test. Correlations were calculated

using a nonparametric Spearman's rank test. Analysis and representation of T-cell function was performed using Simplified Presentation of Incredibly Complex Evaluations (SPICE) v. 6.1, provided by Dr. Mario Roederer (National Institutes of Health, Bethesda, MD).

Acknowledgements

We thank Mr. Hiroyuki Suzuki, Mr. Nobuaki Hatori, and Mr. Kohei Kato of The Research Foundation for Microbial Diseases of Osaka University, for sample storage and management. In addition, we thank all the members of the Laboratory of Immunosenescence, National Institutes of Biomedical Innovation, Health and Nutrition, Osaka, Japan, for their excellent technical support. This study was supported by the Japan Society for the Promotion of Science Grant-in-Aid for Scientific Research (B) (grant number 20H03728) and the Japan Agency for Medical Research and Development (grant numbers 20pc0101047h0001 and 21nf0101627s0202).

Author contributions

TN and TY conceived the study and designed the experiments. TN, KS, YM, MY, MI, YK, and AW performed the experiments and analyzed the data. SM, TK, ST, and YY contributed reagents, materials, and analytical tools. HK and MT conducted patient data and sample collection TN and TY created the figures and wrote the manuscript. All authors verified and discussed the data.

Competing interests

KS and YY are employees of the Research Foundation for Microbial Diseases of Osaka University. The other authors declare no conflicts of interest.

Materials and Correspondence

The data supporting the findings of this study are available from the corresponding author upon request. Source data are provided with this paper.

References

1. Dong, E., Du, H. & Gardner, L. An interactive web-based dashboard to track COVID-19 in real time. *Lancet Infect Dis* **20**, 533-534 (2020).
2. Huang, C. *et al.* Clinical features of patients infected with 2019 novel coronavirus in Wuhan, China. *The Lancet* **395**, 497-506 (2020).
3. Lee, J.S. *et al.* Immunophenotyping of COVID-19 and influenza highlights the role of type I interferons in development of severe COVID-19. *Sci Immunol* **5** (2020).
4. Petersen, E. *et al.* Comparing SARS-CoV-2 with SARS-CoV and influenza pandemics. *The Lancet Infectious Diseases* **20**, e238-e244 (2020).
5. Piroth, L. *et al.* Comparison of the characteristics, morbidity, and mortality of COVID-19 and seasonal influenza: a nationwide, population-based retrospective cohort study. *The Lancet Respiratory Medicine* **9**, 251-259 (2021).
6. Davies, N.G. *et al.* Increased mortality in community-tested cases of SARS-CoV-2 lineage B.1.1.7. *Nature* **593**, 270-274 (2021).
7. Tegally, H. *et al.* Detection of a SARS-CoV-2 variant of concern in South Africa. *Nature* **592**, 438-443 (2021).
8. Wang, P. *et al.* Antibody resistance of SARS-CoV-2 variants B.1.351 and B.1.1.7. *Nature* **593**, 130-135 (2021).
9. Liu, Y. *et al.* Neutralizing Activity of BNT162b2-Elicited Serum. *N Engl J Med* **384**, 1466-1468 (2021).
10. Hoffmann, M. *et al.* SARS-CoV-2 variants B.1.351 and P.1 escape from neutralizing antibodies. *Cell* **184**, 2384-2393 e2312 (2021).
11. Zhou, D. *et al.* Evidence of escape of SARS-CoV-2 variant B.1.351 from natural and vaccine-induced sera. *Cell* **184**, 2348-2361.e2346 (2021).
12. Mlcochova, P. *et al.* SARS-CoV-2 B.1.617.2 Delta variant replication and immune evasion. *Nature* **599**, 114-119 (2021).
13. Karim, S.S.A. & Karim, Q.A. Omicron SARS-CoV-2 variant: a new chapter in the COVID-19 pandemic. *The Lancet* **398**, 2126-2128 (2021).
14. Cameroni, E. *et al.* Broadly neutralizing antibodies overcome SARS-CoV-2 Omicron antigenic shift. *Nature* (2021).
15. Carreño, J.M. *et al.* Activity of convalescent and vaccine serum against SARS-CoV-2 Omicron. *Nature* (2021).
16. Hoffmann, M. *et al.* The Omicron variant is highly resistant against antibody-mediated neutralization – implications for control of the COVID-19 pandemic. *Cell* (2021).
17. Liu, L. *et al.* Striking Antibody Evasion Manifested by the Omicron Variant of SARS-CoV-2. *Nature* (2021).
18. Planas, D. *et al.* Considerable escape of SARS-CoV-2 Omicron to antibody neutralization. *Nature* (2021).
19. Wilfredo F. Garcia-Beltran, K.J.S.D., Angelique Hoelzemer, Evan C. Lam, Adam D. Nitido, Maegan L. Sheehan, Cristhian Berrios, Onosereme Ofoman, Christina C. Chang, Blake M. Hauser, Jared Feldman, Alex L. Roederer, David J. Gregory, Mark C. Poznansky, Aaron G. Schmidt, A. John Iafrate, Vivek Naranbhai, Alejandro B. Balazs mRNA-based COVID-19 vaccine boosters induce neutralizing immunity against SARS-CoV-2 Omicron variant. *Cell* (2021).
20. Dejnirattisai, W. *et al.* SARS-CoV-2 Omicron-B.1.1.529 leads to widespread escape from neutralizing antibody responses. *Cell* (2022).
21. VanBlargan, L.A. *et al.* An infectious SARS-CoV-2 B.1.1.529 Omicron virus escapes neutralization by therapeutic monoclonal antibodies. *Nat Med* (2022).
22. Cao, Y. *et al.* Omicron escapes the majority of existing SARS-CoV-2 neutralizing antibodies. *Nature* (2021).

23. Cheng, S.M.S. *et al.* Neutralizing antibodies against the SARS-CoV-2 Omicron variant following homologous and heterologous CoronaVac or BNT162b2 vaccination. *Nat Med* (2022).
24. Sievers, B.L. *et al.* Antibodies elicited by SARS-CoV-2 infection or mRNA vaccines have reduced neutralizing activity against Beta and Omicron pseudoviruses. *Sci Transl Med*, eabn7842 (2022).
25. Dyer, O. Covid-19: Omicron is causing more infections but fewer hospital admissions than delta, South African data show. *BMJ* **375**, n3104 (2021).
26. Schmidt, M.E. & Varga, S.M. The CD8 T Cell Response to Respiratory Virus Infections. *Front Immunol* **9**, 678 (2018).
27. Pantaleo, G. & Koup, R.A. Correlates of immune protection in HIV-1 infection: what we know, what we don't know, what we should know. *Nat Med* **10**, 806-810 (2004).
28. Rydyznski Moderbacher, C. *et al.* Antigen-Specific Adaptive Immunity to SARS-CoV-2 in Acute COVID-19 and Associations with Age and Disease Severity. *Cell* **183**, 996-1012 e1019 (2020).
29. Tan, A.T. *et al.* Early induction of functional SARS-CoV-2-specific T cells associates with rapid viral clearance and mild disease in COVID-19 patients. *Cell Rep* **34**, 108728 (2021).
30. Tan, L. *et al.* Lymphopenia predicts disease severity of COVID-19: a descriptive and predictive study. *Signal Transduct Target Ther* **5**, 33 (2020).
31. Urra, J.M., Cabrera, C.M., Porras, L. & Rodenas, I. Selective CD8 cell reduction by SARS-CoV-2 is associated with a worse prognosis and systemic inflammation in COVID-19 patients. *Clin Immunol* **217**, 108486 (2020).
32. Sun, J. *et al.* Generation of a Broadly Useful Model for COVID-19 Pathogenesis, Vaccination, and Treatment. *Cell* **182**, 734-743 e735 (2020).
33. McMahan, K. *et al.* Correlates of protection against SARS-CoV-2 in rhesus macaques. *Nature* **590**, 630-634 (2021).
34. Le Bert, N. *et al.* Highly functional virus-specific cellular immune response in asymptomatic SARS-CoV-2 infection. *J Exp Med* **218** (2021).
35. Sahin, U. *et al.* COVID-19 vaccine BNT162b1 elicits human antibody and TH1 T cell responses. *Nature* **586**, 594-599 (2020).
36. Mudd, P.A. *et al.* SARS-CoV-2 mRNA vaccination elicits a robust and persistent T follicular helper cell response in humans. *Cell* (2021).
37. Anderson, E.J. *et al.* Safety and Immunogenicity of SARS-CoV-2 mRNA-1273 Vaccine in Older Adults. *N Engl J Med* **383**, 2427-2438 (2020).
38. Painter, M.M. *et al.* Rapid induction of antigen-specific CD4(+) T cells is associated with coordinated humoral and cellular immunity to SARS-CoV-2 mRNA vaccination. *Immunity* **54**, 2133-2142 e2133 (2021).
39. Tartof, S.Y. *et al.* Effectiveness of mRNA BNT162b2 COVID-19 vaccine up to 6 months in a large integrated health system in the USA: a retrospective cohort study. *The Lancet* **398**, 1407-1416 (2021).
40. Doria-Rose, N. *et al.* Antibody Persistence through 6 Months after the Second Dose of mRNA-1273 Vaccine for Covid-19. *N Engl J Med* **384**, 2259-2261 (2021).
41. Goel, R.R. *et al.* mRNA vaccines induce durable immune memory to SARS-CoV-2 and variants of concern. *Science* **374**, abm0829 (2021).
42. Mateus, J. *et al.* Low-dose mRNA-1273 COVID-19 vaccine generates durable memory enhanced by cross-reactive T cells. *Science* **374**, eabj9853 (2021).
43. Collier, A.-r.Y. *et al.* Immune Responses in Fully Vaccinated Individuals Following Breakthrough Infection with the SARS-CoV-2 Delta Variant in Provincetown, Massachusetts. *medRxiv*, 2021.2010.2018.21265113 (2021).
44. Geers, D. *et al.* SARS-CoV-2 variants of concern partially escape humoral but not T-cell responses in COVID-19 convalescent donors and vaccinees. *Sci Immunol* **6** (2021).
45. Jordan, S.C. *et al.* T cell immune responses to SARS-CoV-2 and variants of concern (Alpha and Delta) in infected and vaccinated individuals. *Cell Mol Immunol* **18**, 2554-2556 (2021).

46. Keeton, R. *et al.* Prior infection with SARS-CoV-2 boosts and broadens Ad26.COV2.S immunogenicity in a variant-dependent manner. *Cell Host Microbe* **29**, 1611-1619 e1615 (2021).
47. Riou, C. *et al.* Escape from recognition of SARS-CoV-2 Beta variant spike epitopes but overall preservation of T cell immunity. *Sci Transl Med*, eabj6824 (2021).
48. Tarke, A. *et al.* Impact of SARS-CoV-2 variants on the total CD4(+) and CD8(+) T cell reactivity in infected or vaccinated individuals. *Cell Rep Med* **2**, 100355 (2021).
49. Keeton, R. *et al.* SARS-CoV-2 spike T cell responses induced upon vaccination or infection remain robust against Omicron. *medRxiv*, 2021.2012.2026.21268380 (2021).
50. Tarke, A. *et al.* SARS-CoV-2 vaccination induces immunological T cell memory able to cross-recognize variants from Alpha to Omicron. *Cell* (2022).
51. Liu, J. *et al.* Vaccines Elicit Highly Conserved Cellular Immunity to SARS-CoV-2 Omicron. *Nature* (2022).
52. Gao, Y. *et al.* Ancestral SARS-CoV-2-specific T cells cross-recognize the Omicron variant. *Nat Med* (2022).
53. Barry, M. & Bleackley, R.C. Cytotoxic T lymphocytes: all roads lead to death. *Nat Rev Immunol* **2**, 401-409 (2002).
54. Berke, G. The CTL's kiss of death. *Cell* **81**, 9-12 (1995).
55. Naaber, P. *et al.* Dynamics of antibody response to BNT162b2 vaccine after six months: a longitudinal prospective study. *Lancet Reg Health Eur* **10**, 100208 (2021).
56. Ahmadi, P. *et al.* Defining the CD39/CD73 Axis in SARS-CoV-2 Infection: The CD73(-) Phenotype Identifies Polyfunctional Cytotoxic Lymphocytes. *Cells* **9** (2020).
57. Mazzoni, A. *et al.* Impaired immune cell cytotoxicity in severe COVID-19 is IL-6 dependent. *J Clin Invest* **130**, 4694-4703 (2020).
58. Li, M. *et al.* Elevated Exhaustion Levels of NK and CD8(+) T Cells as Indicators for Progression and Prognosis of COVID-19 Disease. *Front Immunol* **11**, 580237 (2020).
59. Habel, J.R. *et al.* Suboptimal SARS-CoV-2-specific CD8(+) T cell response associated with the prominent HLA-A*02:01 phenotype. *Proc Natl Acad Sci U S A* **117**, 24384-24391 (2020).
60. Harari, A., Bellutti Enders, F., Cellerai, C., Bart, P.A. & Pantaleo, G. Distinct profiles of cytotoxic granules in memory CD8 T cells correlate with function, differentiation stage, and antigen exposure. *J Virol* **83**, 2862-2871 (2009).
61. De Biasi, S. *et al.* Marked T cell activation, senescence, exhaustion and skewing towards TH17 in patients with COVID-19 pneumonia. *Nat Commun* **11**, 3434 (2020).
62. Song, J.W. *et al.* Immunological and inflammatory profiles in mild and severe cases of COVID-19. *Nat Commun* **11**, 3410 (2020).
63. Zheng, H.Y. *et al.* Elevated exhaustion levels and reduced functional diversity of T cells in peripheral blood may predict severe progression in COVID-19 patients. *Cell Mol Immunol* **17**, 541-543 (2020).
64. Rha, M.S. *et al.* PD-1-Expressing SARS-CoV-2-Specific CD8(+) T Cells Are Not Exhausted, but Functional in Patients with COVID-19. *Immunity* **54**, 44-52 e43 (2021).

Table.1 | Donor characteristics enrolled in this study

Caracteristics	Mild (n = 9)	Moderate I (n = 11)	Moderate II/Severe (n = 10)	Vaccinated donors (n = 21)
Demographic				
Age, median years (interquartile range)	62 (48 - 69)	70 (53 - 76.5)	64.5 (49.25 - 72.75)	39 (26-52)
Male (%)	6 (66.7)	5 (45.5)	8 (80.0)	6 (28.6)
Female (%)	3 (33.3)	6 (54.5)	2 (20.0)	15 (71.4)
Time since sympton onset median days (interquartile range)	4 (4-6)	8 (4.5-11.5)	7 (7-8)	NA
Days to recovery median days (interquartile range)	15 (13-15)	22 (16-34)	19 (17-20)	NA
Presenting Symptoms				
Fever no. (%)	6 (66.7)	6 (54.5)	6 (60.0)	NA
Cough no. (%)	3 (33.3)	7 (63.6)	6 (60.0)	NA
Dyspnea no. (%)	1 (11.1)	6 (54.5)	5 (50.0)	NA
Rhinorrhea no. (%)	0 (0)	3 (27.3)	1 (10.0)	NA
Sore throat no. (%)	3 (33.3)	0 (0)	1 (10.0)	NA
Diarrhea no. (%)	0 (0)	1 (9.1)	2 (20.0)	NA
Hematological values (Median, Interquartile range)				
Haemoglobin (g/dL)	14.1 (13.1-14.6)	14.1 (12.45-14.8)	14.9 (14.375-15.25)	NA
WBC ($x10^9$/L)	5.5 (4.4-6.4)	5.3 (3.4-6.8)	4.1 (2.6-5.9)	NA
Lymphocytes ($x10^9$/L)	25.2 (18.8-27.8)	19.5 (17.15-24.75)	24.5 (22-29.7)	NA
Neutrophil ($x10^9$/L)	66.0 (64.4-70.4)	71.4 (66.25-74.8)	66.7 (58.725-73.375)	NA
Platelet ($x10^9$/L)	177 (156-189)	201 (133-216.5)	183.5 (132-200)	NA

Figure legends

Figure 1. Acute-phase SARS-CoV-2 spike-specific $CD8^+$ T-cell response is associated with COVID-19 severity.

(a) Percentage of anti-spike (Alpha) IgG endpoint titer as a function of viral load (n = 30). **(b)** Dot plot representing the anti-spike (Alpha) IgG end-point titer in plasma samples of patients with acute mild (n = 9), acute moderate I (n = 11), or acute moderate II/severe (n = 10) disease. The lines show the geometric mean. **(c)** Representative flow cytometry data showing $CD69^+$4-$1BB^+$ $CD8^+$ T cells as SARS-CoV-2 (Alpha) spike-specific $CD8^+$ T cells. The numbers show the frequencies of $CD69^+$4-$1BB^+$ $CD8^+$ T cells in $CD8^+$ total memory cells. **(d)** Percentage of $CD69^+$4-$1BB^+$ $CD8^+$ T cells after background subtraction (control DMSO) as a function of viral load. **(e)** Frequencies of $CD69^+$4-$1BB^+$ $CD8^+$ T cells of patients with acute mild, acute moderate I, or acute moderate II/severe disease. The lines show the geometric mean. P-values were calculated using the nonparametric Mann-Whitney U test.

Figure 2. Functional characteristics of SARS-CoV-2 spike-specific $CD8^+$ T cells in acute COVID-19.

(a) Dot plots representing the frequencies of IFN-γ-, TNF-, or IL-2-secreting $CD8^+$ T cells (left, center, and right panels, respectively) responding to SARS-CoV-2 Alpha spike peptides in $CD8^+$ total memory cells. The lines show the geometric means. **(b)** Frequencies of spike-specific $CD8^+$ T cell subpopulations producing IFN-γ, TNF, and IL-2 in cytokine secreting $CD8^+$ total memory cells (n = 23). **(c)** Dot plots representing the frequencies of $CD69^+$4-$1BB^+CD8^+$ T cells expressing granzyme A (left panel), granzyme B (center panel), or perforin (right panel) responding to SARS-CoV-2 Alpha spike peptides (n = 23). The lines show the geometric means. **(d)** Frequencies of spike-specific $CD69^+$4-$1BB^+CD8^+$ T cell subpopulations expressing different combinations of granzyme A, granzyme B, and perforin (n = 23). P-values were calculated using the nonparametric Mann-Whitney U test. *$P < 0.05$. **(e)** Frequency of spike-specific $CD69^+$4-$1BB^+CD8^+$ T cells with wide-spectrum

cytotoxicity expressing granzyme A, granzyme B, and perforin. *P*-values were calculated using permutation tests.

Figure 3. Antibody and $CD4^+$ T cells induced by mRNA vaccine against SARS-CoV-2 variants of concern.

(a) Anti-spike IgG against WT (left panel), Delta (center panel), and Omicron (right panel) endpoint titers over time in plasma samples obtained from BNT162b2-vaccinated individuals (n = 21). *P*-values were calculated using the Wilcoxon matched-pairs signed rank test. **(b)** Comparison of anti-spike IgG endpoint titer against WT, Delta, and Omicron spike proteins at four and twelve weeks post-second vaccination (n = 21). *P*-values were calculated using the Wilcoxon matched-pairs signed rank test. **(c)** Comparison of spike-specific Th1 cell frequency against WT, Delta, and Omicron spike peptides in $CD4^+$ total memory cells at four and twelve weeks post-second vaccination (n = 21). *P*-values were calculated using the Wilcoxon matched-pairs signed rank test. **(d)** Correlation of anti-spike IgG endpoint titer and spike-specific Th1 cell frequency against WT (black), Delta (blue), and Omicron (red) spike peptides (n = 21). Correlations were calculated using the nonparametric Spearman's rank test.

Figure 4. $CD8^+$ T cells induced by mRNA vaccine against SARS-CoV-2 variants of concern.

(a) Dot plot representing the frequencies of $CD69^+4\text{-}1BB^+$ $CD8^+$ T cells in $CD8^+$ total memory cells with subtracted background (control DMSO) of cells obtained from vaccinated healthy individuals (n = 21). The lines show the geometric mean. **(b)** Frequencies of $CD69^+4\text{-}1BB^+CD8^+$ T cells expressing granzyme A (left panels), granzyme B (center panels), or perforin (right panels) responding to SARS-CoV-2 WT, Delta, or Omicron spike peptides (upper, middle, and lower panels, respectively) (WT, 4 weeks, n = 13; WT, 12 weeks, n = 15; Delta, 4 weeks, n = 12; Delta, 12 weeks, n = 13; Omicron, 4 weeks, n = 15; Omicron, 12 weeks, n = 13). Lines show medians. *P*-values were calculated using the Wilcoxon matched-pairs signed rank test. **(c)** Frequencies of spike-specific $CD69^+4\text{-}1BB^+CD8^+$ T cell subpopulations expressing different combination of granzyme A, granzyme B, and perforin. *P*-values were calculated using the Wilcoxon matched-pairs signed rank test. **(d)** Frequency of polyfunctional

spike-specific $CD69^{+}4\text{-}1BB^{+}CD8^{+}$ T cells expressing granzyme A, granzyme B, and perforin. *P*-values were calculated using permutation tests.

Figure 1

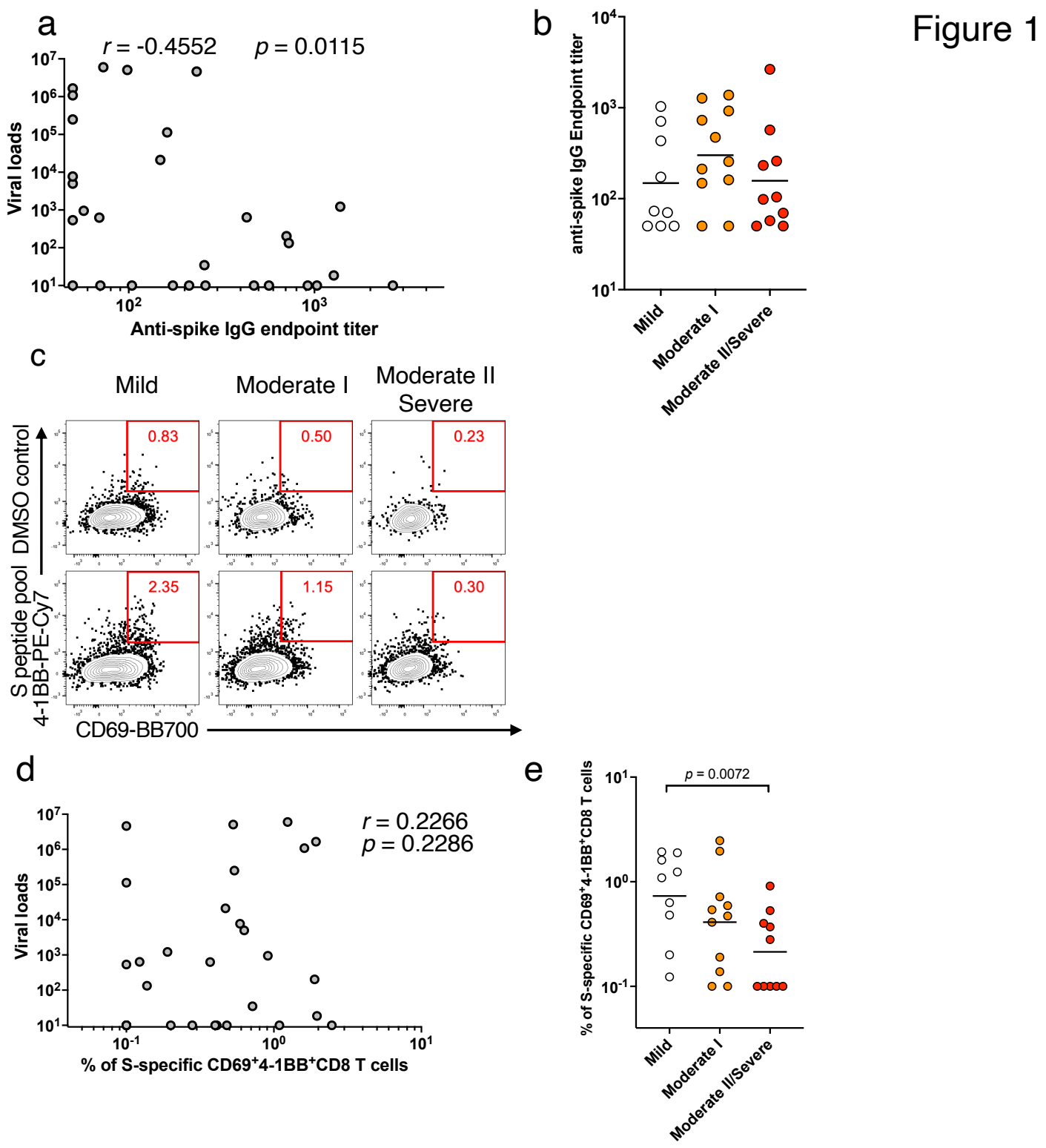

Figure 1. Acute-phase SARS-CoV-2 spike-specific CD8⁺ T-cell response is associated with COVID-19 severity. **(a)** Percentage of anti-spike (Alpha) IgG endpoint titer as a function of viral load (n = 30). **(b)** Dot plot representing the anti-spike (Alpha) IgG end-point titer in plasma samples of patients with acute mild (n = 9), acute moderate I (n = 11), or acute moderate II/severe (n = 10) disease. The lines show the geometric mean. **(c)** Representative flow cytometry data showing CD69⁺4-1BB⁺ CD8⁺ T cells as SARS-CoV-2 (Alpha) spike-specific CD8⁺ T cells. The numbers show the frequencies of CD69⁺4-1BB⁺ CD8⁺ T cells in CD8⁺ total memory cells. **(d)** Percentage of CD69⁺4-1BB⁺ CD8⁺ T cells after background subtraction (control DMSO) as a function of viral load. **(e)** Frequencies of CD69⁺4-1BB⁺ CD8⁺ T cells of patients with acute mild, acute moderate I, or acute moderate II/severe disease. The lines show the geometric mean. *P*-values were calculated using the nonparametric Mann-Whitney *U* test.

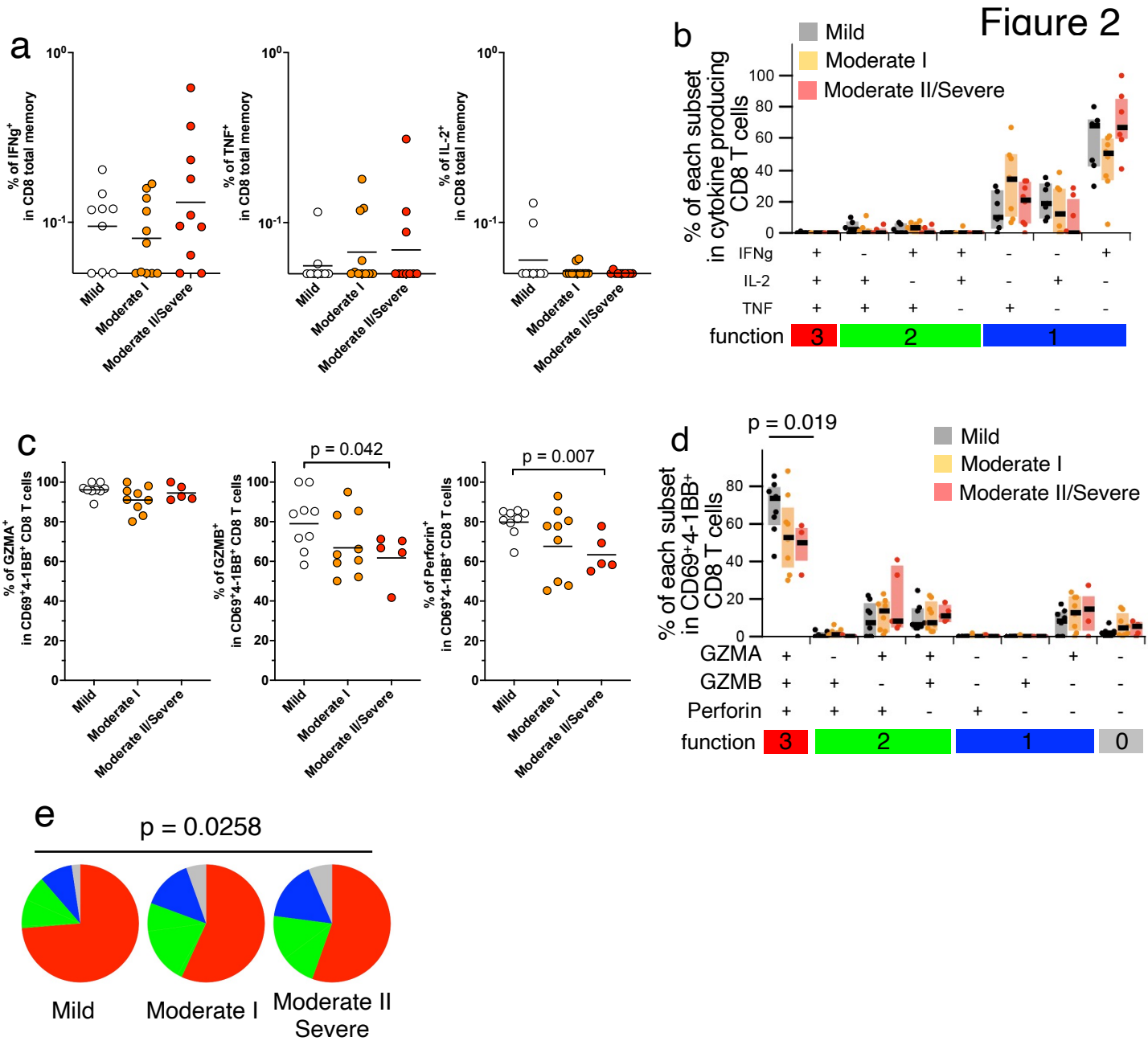

Figure 2. Functional characteristics of SARS-CoV-2 spike-specific CD8⁺ T cells in acute COVID-19.
(a) Dot plots representing the frequencies of IFN-γ-, TNF-, or IL-2-secreting CD8⁺ T cells (left, center, and right panels, respectively) responding to SARS-CoV-2 Alpha spike peptides in CD8⁺ total memory cells. The lines show the geometric means. **(b)** Frequencies of spike-specific CD8⁺ T cell subpopulations producing IFN-γ, TNF, and IL-2 in cytokine secreting CD8⁺ total memory cells ($n = 23$). **(c)** Dot plots representing the frequencies of CD69⁺4-1BB⁺CD8⁺ T cells expressing granzyme A (left panel), granzyme B (center panel), or perforin (right panel) responding to SARS-CoV-2 Alpha spike peptides ($n = 23$). The lines show the geometric means. **(d)** Frequencies of spike-specific CD69⁺4-1BB⁺CD8⁺ T cell subpopulations expressing different combinations of granzyme A, granzyme B, and perforin ($n = 23$). *P*-values were calculated using the nonparametric Mann-Whitney *U* test. $*P < 0.05$.
(e) Frequency of spike-specific CD69⁺4-1BB⁺CD8⁺ T cells with wide-spectrum cytotoxicity expressing granzyme A, granzyme B, and perforin. *P*-values were calculated using permutation tests.

Figure 3

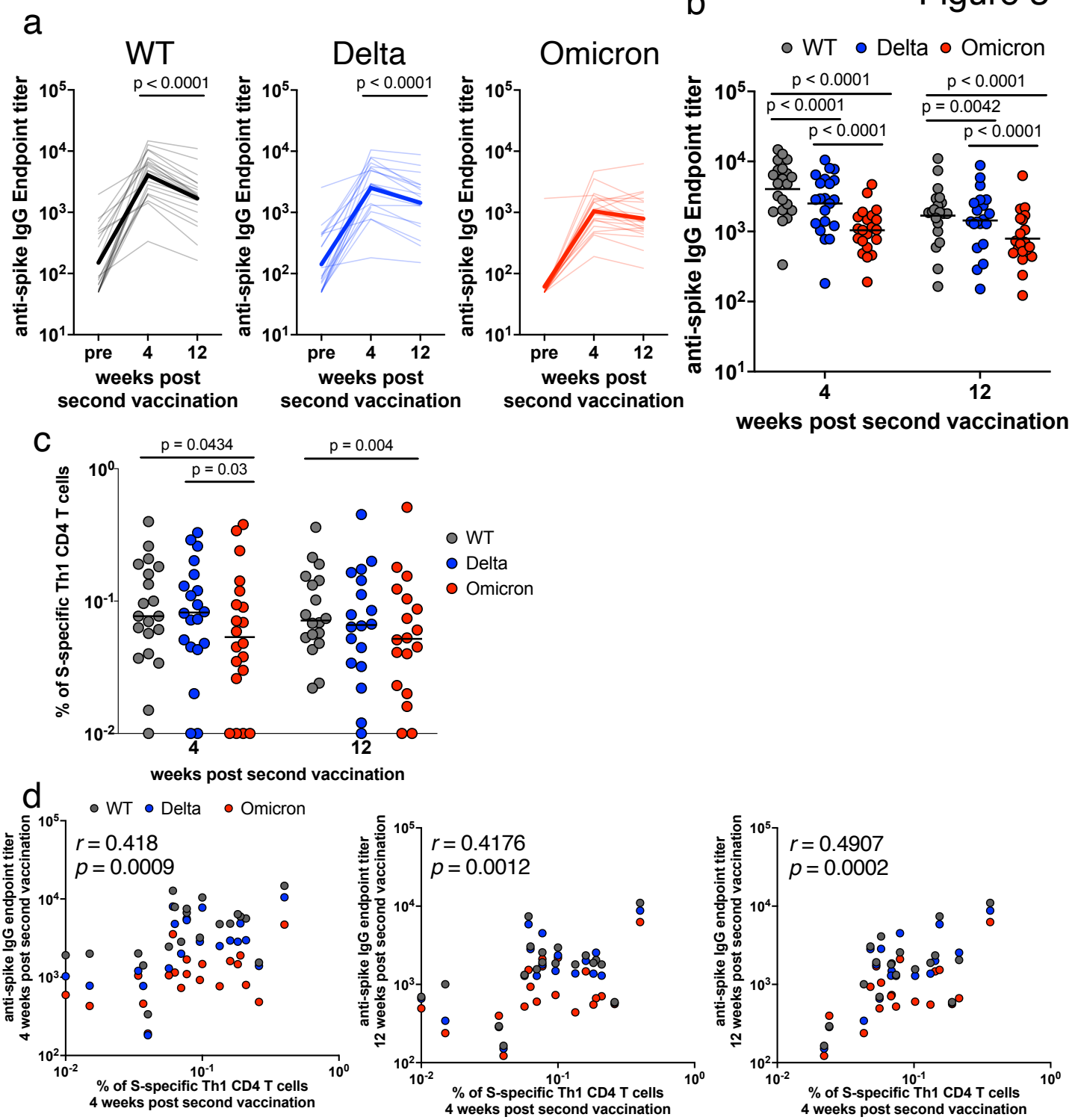

Figure 3. Antibody and CD4⁺ T cells induced by mRNA vaccine against SARS-CoV-2 variants of concern. **(a)** Anti-spike IgG against WT (left panel), Delta (center panel), and Omicron (right panel) endpoint titers over time in plasma samples obtained from BNT162b2-vaccinated individuals ($n = 21$). *P*-values were calculated using the Wilcoxon matched-pairs signed rank test. **(b)** Comparison of anti-spike IgG endpoint titer against WT, Delta, and Omicron spike proteins at four and twelve weeks post-second vaccination ($n = 21$). *P*-values were calculated using the Wilcoxon matched-pairs signed rank test. **(c)** Comparison of spike-specific Th1 cell frequency against WT, Delta, and Omicron spike peptides in CD4⁺ total memory cells at four and twelve weeks post-second vaccination ($n = 21$). *P*-values were calculated using the Wilcoxon matched-pairs signed rank test. **(d)** Correlation of anti-spike IgG endpoint titer and spike-specific Th1 cell frequency against WT (black), Delta (blue), and Omicron (red) spike peptides ($n = 21$). Correlations were calculated using the nonparametric Spearman's rank test.

Figure 4

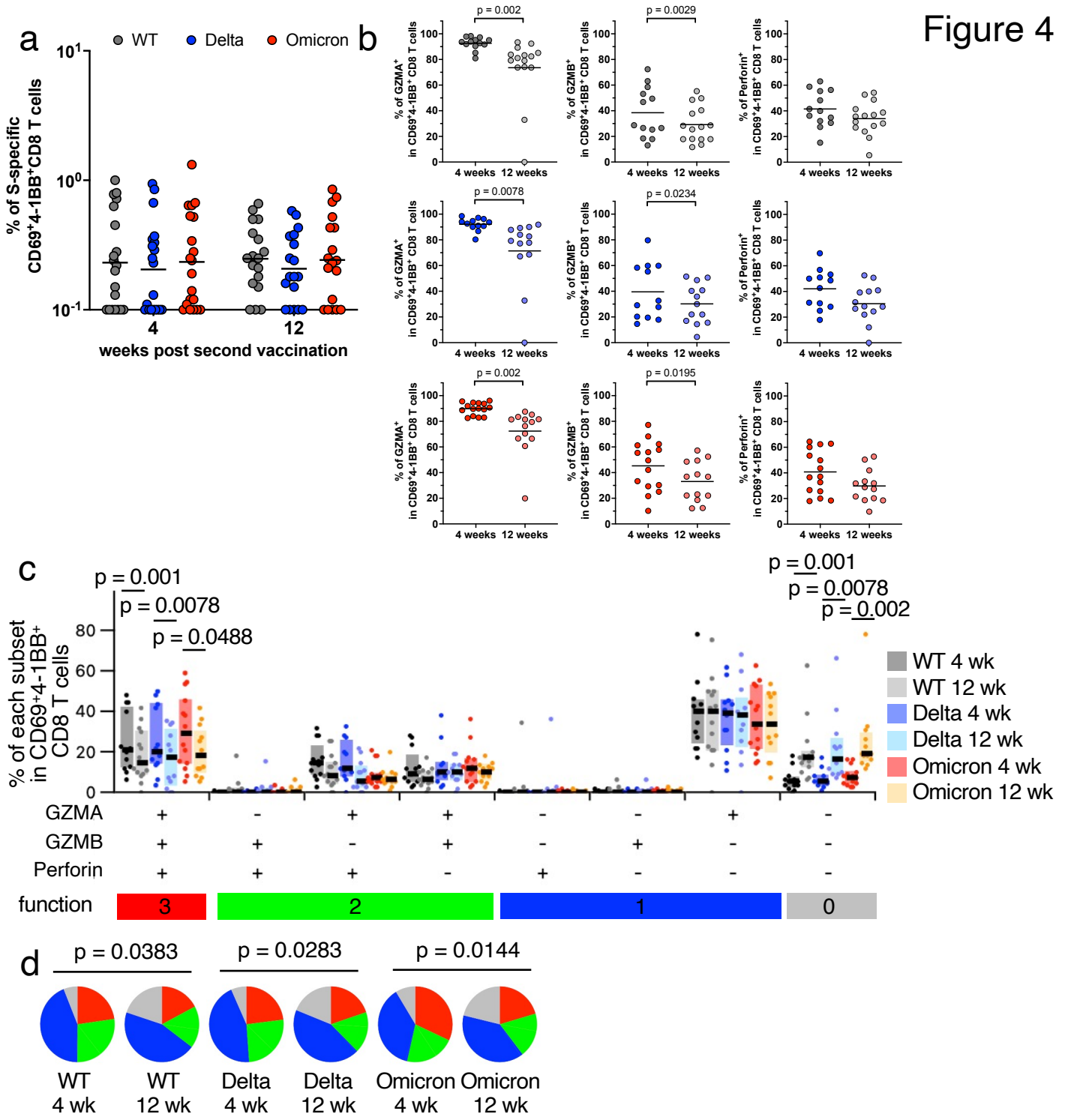

Figure 4. CD8⁺ T cells induced by mRNA vaccine against SARS-CoV-2 variants of concern.
(a) Dot plot representing the frequencies of CD69⁺4-1BB⁺ CD8⁺ T cells in CD8⁺ total memory cells with subtracted background (control DMSO) of cells obtained from vaccinated healthy individuals (n = 21). The lines show the geometric mean. **(b)** Frequencies of CD69⁺4-1BB⁺CD8⁺ T cells expressing granzyme A (left panels), granzyme B (center panels), or perforin (right panels) responding to SARS-CoV-2 WT, Delta, or Omicron spike peptides (upper, middle, and lower panels, respectively) (WT, 4 weeks, n = 13; WT, 12 weeks, n = 15; Delta, 4 weeks, n = 12; Delta, 12 weeks, n = 13; Omicron, 4 weeks, n = 15; Omicron, 12 weeks, n = 13). Lines show medians. *P*-values were calculated using the Wilcoxon matched-pairs signed rank test. **(c)** Frequencies of spike-specific CD69⁺4-1BB⁺CD8⁺ T cell subpopulations expressing different combination of granzyme A, granzyme B, and perforin. *P*-values were calculated using the Wilcoxon matched-pairs signed rank test. **(d)** Frequency of polyfunctional spike-specific CD69⁺4-1BB⁺CD8⁺ T cells expressing granzyme A, granzyme B, and perforin. *P*-values were calculated using permutation tests.

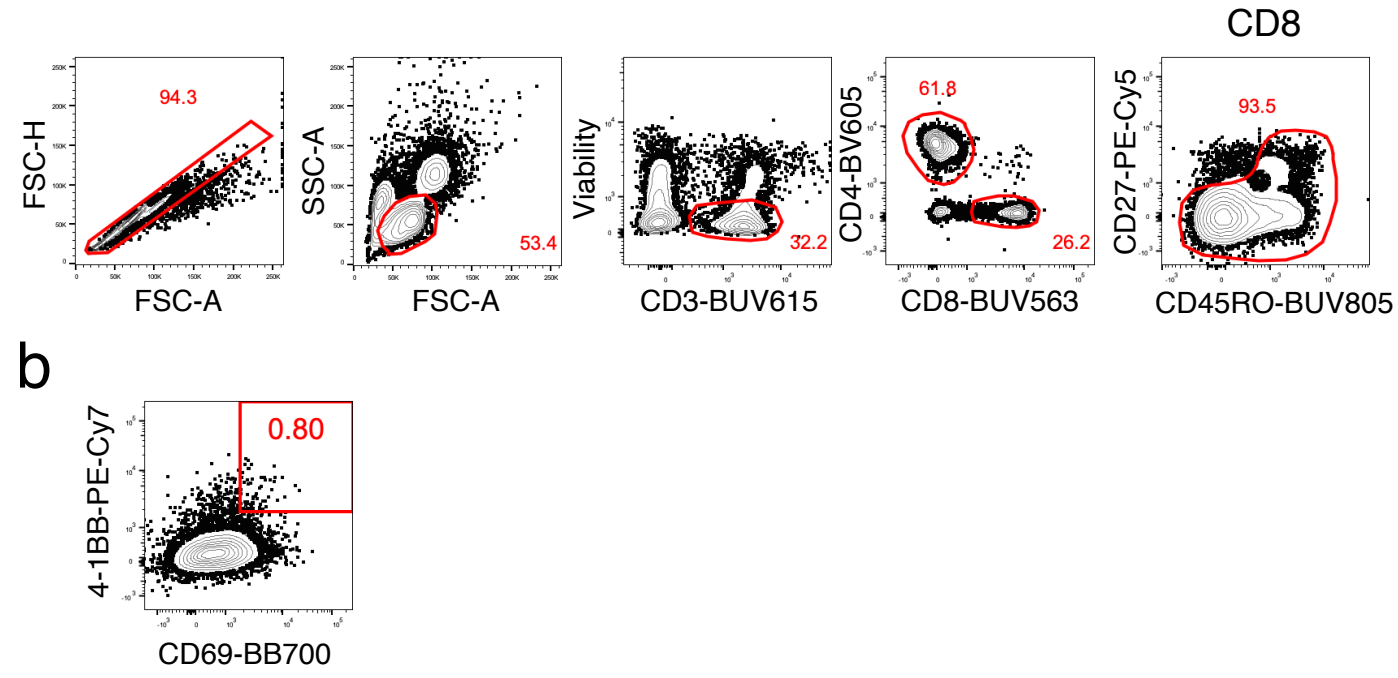

Extended Data Fig. 1 | Gating strategy for antigen-specific CD8 T cells (related to Figure 1). **(a)** After gating live single T cells, based on forward scatter area and height (FSC-A and -H), side scatter area (SSC-A), live/dead cell exclusion, and CD3 staining, we separated the peripheral blood mononuclear cells (PBMCs) into $CD4^+$ and $CD8^+$ T cells. Subsequently, $CD8^+$ T cells were further divided into memory phenotypes based on the expression of CD27 and CD45RO. **(b)** After gating $CD8^+$ memory T cells, SARS-CoV-2 spike-specific $CD8^+$ T cells were defined as the $CD69^+4\text{-}1BB^+$ population.

Extended Data Figure 2

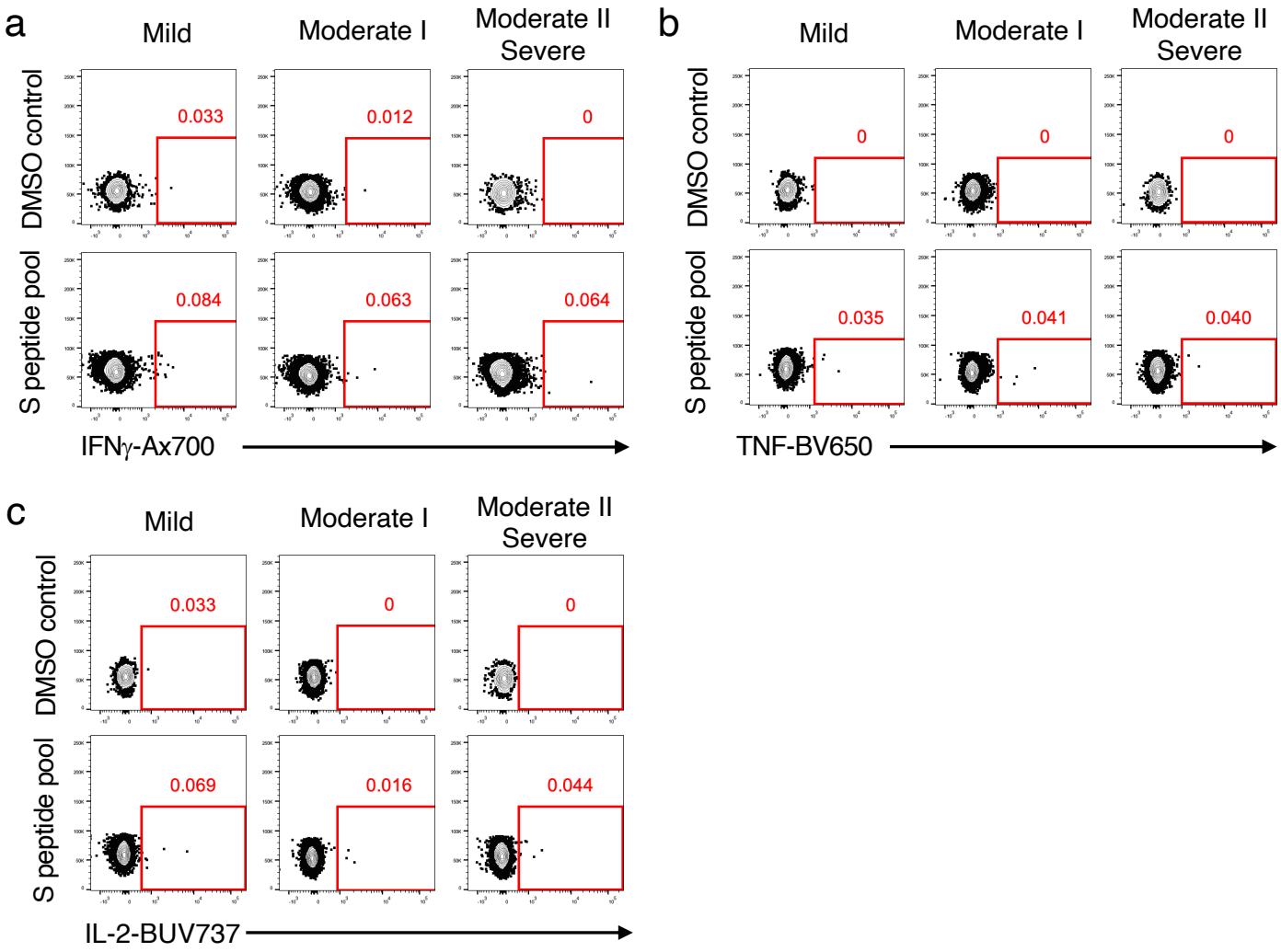

Extended Data Fig. 2 | Gating strategy for antigen-specific CD8 T cells (related to Figure 2). Peripheral blood mononuclear cells (PBMCs) obtained from SARS-CoV-2-infected patients were either not stimulated (DMSO control) or stimulated with SARS-CoV-2 (Alpha) spike peptides for 6 h. Representative plots of (**a**) IFN-γ, (**b**) TNF, and (**c**) IL-2 production from $CD8^+$ memory T cells.

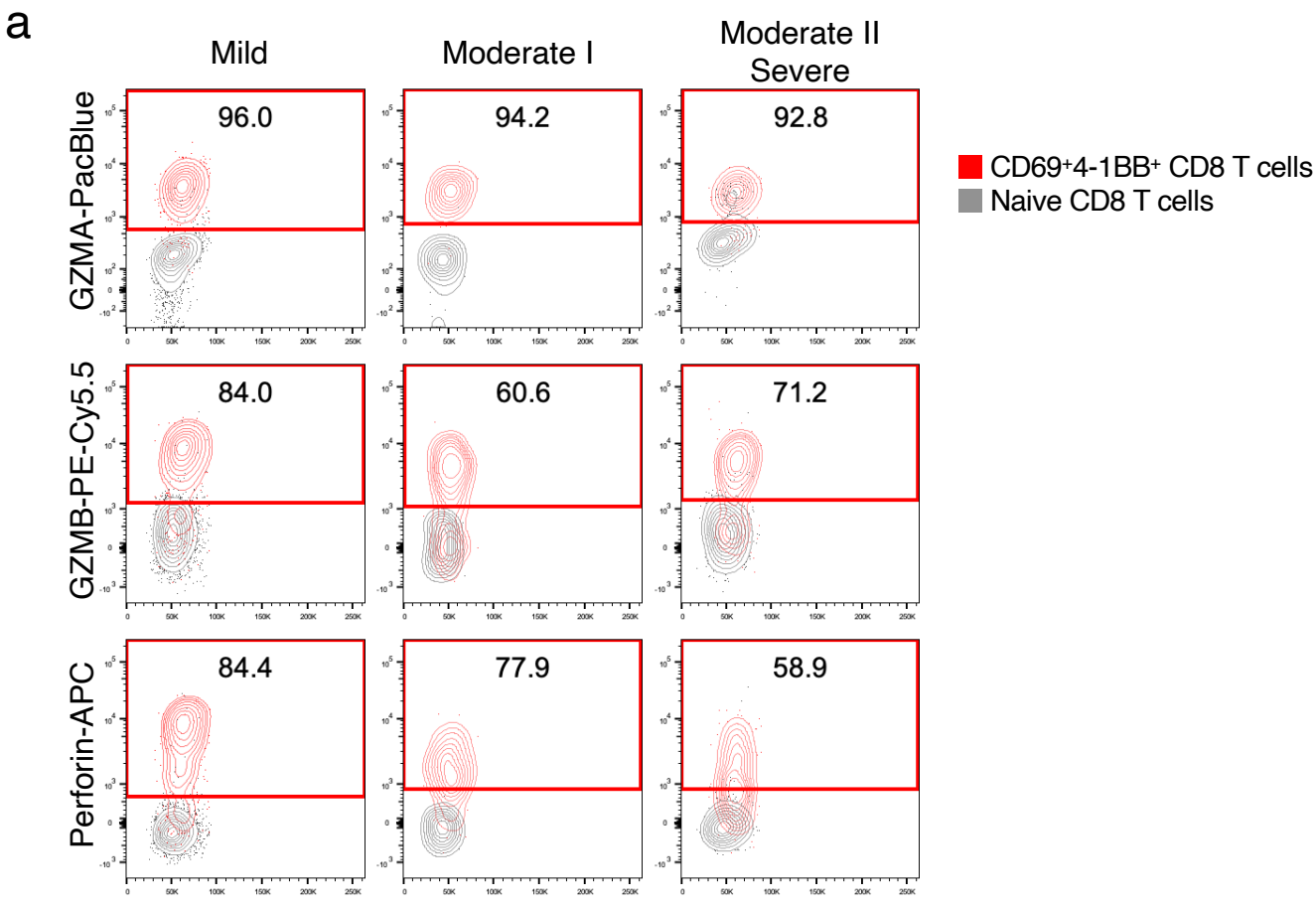

Extended Data Fig. 3 | Gating strategy for antigen-specific CD8 T cells (related to Figure 2). Representative plots of granzyme A (GZMA), granzyme B (GZMB) and perforin expression in $CD69^{+}4\text{-}1BB^{+}CD8^{+}$ memory T cells from patients. The gray contour plots represent the expression of each cytotoxic molecule in $CD8^{+}$ naive T cells.

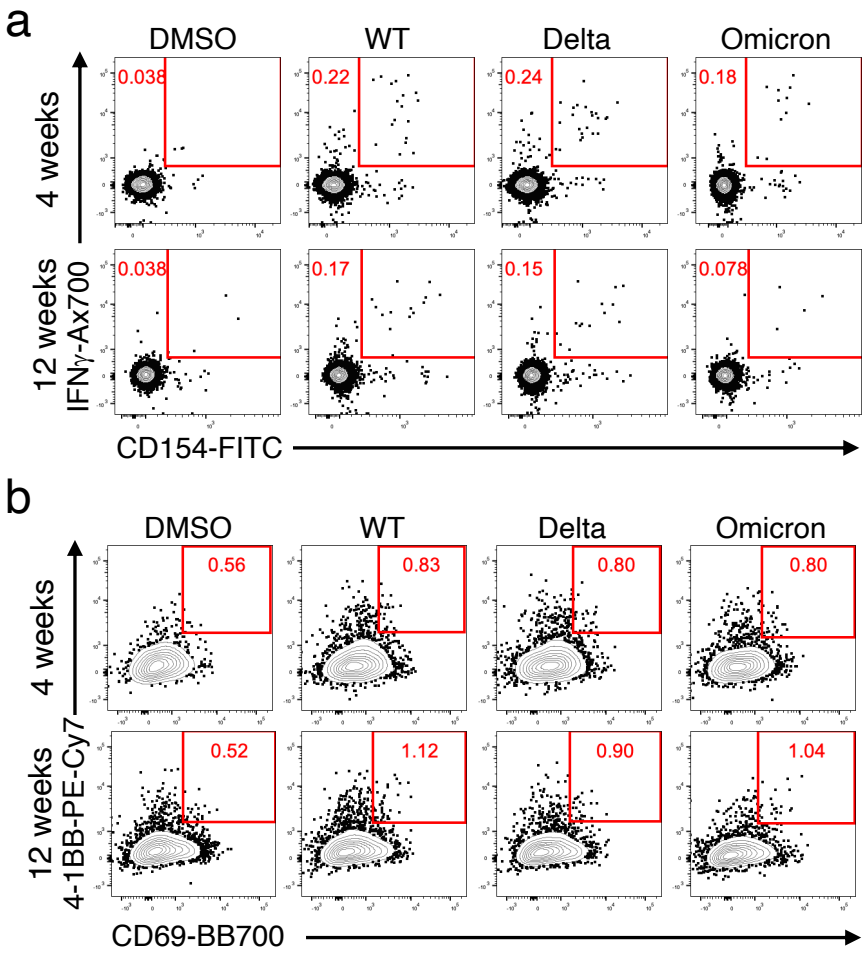

Extended Data Fig. 4 | Gating strategy for antigen-specific CD4 and CD8 T cells (related to Figures 3 and 4).

(**a**) Peripheral blood mononuclear cells (PBMCs) obtained from BNT162b2-vaccinated healthy individuals at four and twelve weeks post-second vaccination were either not stimulated (DMSO control) or stimulated with SARS-CoV-2 spike peptides (WT, Delta, or Omicron) for 6 h. Th1 cells were defined as $CD154^{+}IFN\text{-}\gamma^{+}CD4^{+}$ memory T cells. (**b**) SARS-CoV-2 spike-specific $CD8^{+}$ T cells from BNT162b2-vaccinated healthy individuals were identified as in Extended Data Figure 1.

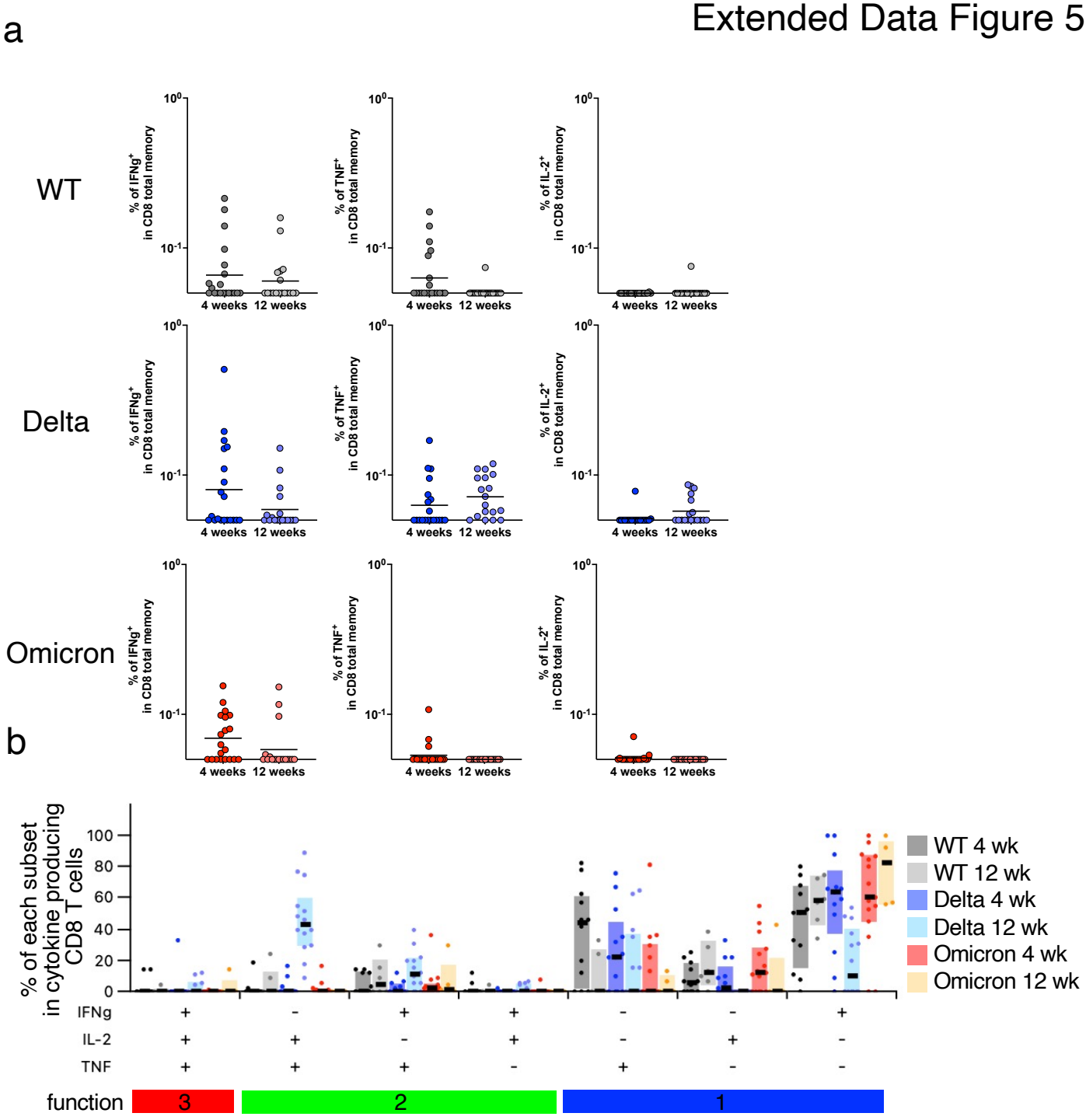

Extended Data Fig. 5 | Functional characteristics of SARS-CoV-2 spike-specific CD8⁺ T cells from vaccinated donors.

(**a**) Frequencies of IFN-γ-, TNF-, or IL-2-producing CD8⁺ T cells (upper, middle, and lower panels, respectively) responding to SARS-CoV-2 spike peptides in CD8⁺ total memory cells from BNT162b2-vaccinated healthy individuals. The lines show the geometric means. (**b**) Frequencies of subpopulations of spike-specific CD8⁺ T cells producing IFN-γ, TNF, and IL-2 in cytokine-secreting CD8⁺ total memory cells.

Supplementary Files

This is a list of supplementary files associated with this preprint. Click to download.

- SupplementaryTable1.xlsx